Multibody System Dynamics
https://doi.org/10.1007/s11044-025-10093-x

REVIEW

Galerkin-based time integration approaches to rigid body dynamics in terms of unit quaternions

Marvin May[1] · **Peter Betsch**[1]

Received: 1 April 2025 / Accepted: 30 June 2025

Abstract
Galerkin-based time integration approaches are investigated for discrete mechanical systems subject to holonomic constraints. In this connection, rigid body rotations are described by using unit quaternions, resulting in a configuration-dependent mass matrix. Two different Galerkin methods are developed: (i) a Petrov-Galerkin approach leading to the common time-stepping format of numerical integrators for initial value problems and (ii) a Bubnov-Galerkin method leading to a global solution procedure. The numerical performance of the alternative schemes is compared, including their algorithmic conservation properties, accuracy, and satisfaction of the constraints on configuration and velocity level. The global Galerkin-based approach is deemed to be advantageous for the solution of inverse dynamics and optimal control problems, in which a flow of information backwards in time is required. Numerical examples involving large rotations are investigated to assess the numerical performance of the alternative Galerkin approaches. In addition to that, a comparison of the quaternion-based rigid body formulation with a director-based formulation is included.

Keywords Galerkin methods · Rotation parameterization · Rigid body dynamics

1 Introduction

Time-stepping schemes for the numerical integration of rigid body dynamics are often based on finite difference schemes, which emanate from the strong form of the equations of motion and are well studied. For example, the Euler equations of rigid body dynamics lie at the heart of the conserving schemes proposed in [17, 23] and [15].

The choice of coordinates for the parametrization of the rotation manifold plays a major role in the design of time integration schemes for rigid body dynamics. For example, one may use minimal coordinates such as Euler angles or redundant coordinates such as unit quaternions. Alternatively, rotations can be described by using three directors which constitute a time-dependent orthogonal basis fixed to the rigid body and rotating with it. Due to the fact that Euler angles exhibit singularities, which may lead to numerical instabilities, unit quaternions and director triads are often used to describe rigid body dynamics. Although this

✉ M. May
marvin.may2@kit.edu

[1] Institute of Mechanics, Karlsruhe Institute of Technology (KIT), Otto-Ammann-Platz 9, 76131 Karlsruhe, Germany

Published online: 21 July 2025

approach circumvents singularity-related problems such as gimbal lock, it requires solving differential-algebraic equations (DAEs) rather than ordinary differential equations (ODEs). The DAEs originate from internal constraints which impose the condition of rigidity. In the case of unit quaternions one has to impose one internal constraint associated with the unit-length condition for the quaternion. If the director triad is used, six independent internal constraints are required to ensure that the director triad remains orthonormal.

In addition to the internal constraints, external constraints can be used to describe general multibody systems. Thus the DAE-based formulation of rigid body dynamics constitutes a general framework for the description of arbitrarily complex multibody systems including closed kinematic loops.

Unit quaternions (also called Euler parameters) have been used in the pioneering works by Haug and Nikravesh, see [10, 21] and also [22]. Later on, structure-preserving time-stepping schemes based on unit-quaternions have been developed in the Lagrangian framework by [26] and in the Hamiltonian framework by [2] and [20]. Similarly, structure-preserving time-stepping schemes relying on the director triad have been proposed by [18] and [4].

While quaternions are less redundant compared to the director formulation, they introduce a configuration-dependent mass matrix, which can complicate the numerical integration of the equations of motion. Moreover, this mass matrix is inherently singular, which poses challenges in the Hamiltonian framework, where the inverse mass matrix is required. It is worth noting that the issue of a singular mass-matrix can be avoided by resorting to the Livens principle as has been shown recently in [12]. Another potential issue is the non-uniqueness of unit quaternions, which can cause so-called unwinding phenomena when solving control problems [7]. However, the non-uniqueness of unit quaternions typically does not cause any problems in the application of time-stepping schemes.

In contrast to the time-marching procedure typically applied to solve initial value problems, global time integration approaches provide an alternative avenue to solve both initial value problems and boundary value problems. These boundary value problems might be related to inverse dynamics problems [25] and optimal control problems [9].

A Galerkin-based global time integration method has been recently proposed for rigid body initial value problems in [11]. In this work the director-based formulation of rigid bodies has been applied. In the present work we propose a similar Galerkin-based global time integration method relying on the unit-quaternion representation of rigid bodies. Since the global approach covers the complete time interval of interest, it naturally leads to a large algebraic system of equations to be solved. Thus the lower degree of redundancy of unit quaternions leads to a significant reduction of unknowns when compared to the director-based formulation of rigid bodies.

While the global time integration method can be classified as Bubnov-Galerkin method, there exists also a Petrov-Galerkin variant. Due to the use of discontinuous test functions, the Petrov-Galerkin formulation facilitates the design of time-stepping schemes. Besides the global Bubnov-Galerkin method in terms of unit quaternions we also present a Petrov-Galerkin variant recovering the common time-stepping format for initial value problems. Accordingly, in the present work we newly propose both a global Bubnov-Galerkin method and a Petrov-Galerkin method for the solution of rigid body initial value problems relying on the use of unit-quaternions.

The rest of this work is structured as follows. In Sect. 2 we summarize both the Lagrangian and the Hamiltonian framework for the description of mechanical systems subject to holonomic constraints. The Galerkin-based approach to the solution of initial value problems is described in Sect. 3. The alternative parametrization of rigid motion in terms of

unit quaternions and director triads is covered in Sect. 4. After the numerical investigations presented in Sect. 5, conclusions are drawn in Sect. 6.

2 Holonomically constrained mechanical systems

Consider a conservative mechanical system with n coordinates collected in $\mathbf{q}(t) \in \mathbb{R}^n$ and m scleronomic and holonomic constraints $\mathbf{\Phi} : \mathbb{R}^n \to \mathbb{R}^m$. The configuration space Q of the constrained mechanical system is given by

$$Q = \{\mathbf{q} \in \mathbb{R}^n | \mathbf{\Phi}(\mathbf{q}) = \mathbf{0}\}. \tag{1}$$

The associated velocities $\dot{\mathbf{q}}(t) = \frac{\mathrm{d}}{\mathrm{d}t}\mathbf{q}(t)$ belong to the tangent space $T_{\mathbf{q}}Q$ at $\mathbf{q}(t) \in Q$ defined by

$$T_{\mathbf{q}}Q = \{\dot{\mathbf{q}} \in \mathbb{R}^n | \mathbf{\Psi}(\mathbf{q}, \dot{\mathbf{q}}) = \mathbf{0}\}, \tag{2}$$

where $\mathbf{\Psi}(\mathbf{q}, \dot{\mathbf{q}}) = \frac{\mathrm{d}}{\mathrm{d}t}\mathbf{\Phi}(\mathbf{q})$ defines the hidden constraint on the velocity level. Correspondingly, $(\mathbf{q}, \dot{\mathbf{q}}) \in TQ$, the velocity phase space. The dynamics of the constrained mechanical system is governed by Hamilton's principle for constrained systems [19]

$$\delta\tilde{S} = \int_{t_0}^{t_f} \delta L_{\boldsymbol{\gamma}} \, \mathrm{d}t = 0, \tag{3}$$

where $L_{\boldsymbol{\gamma}}$ denotes the augmented Lagrangian of the form

$$L_{\boldsymbol{\gamma}} = L - \boldsymbol{\gamma} \cdot \mathbf{\Phi}. \tag{4}$$

Here, $L : TQ \to \mathbb{R}$ is the Lagrange function and $\boldsymbol{\gamma} \in \mathbb{R}^m$ is a vector of Lagrange multipliers. The Euler-Lagrange equations emanating from (3) correspond to Lagrange's equations of the first kind

$$\begin{aligned} \frac{\mathrm{d}}{\mathrm{d}t}\left(\nabla_{\dot{\mathbf{q}}} L\right) - \nabla_{\mathbf{q}} L + \nabla_{\mathbf{q}} \mathbf{\Phi}^T \boldsymbol{\gamma} &= \mathbf{0} \\ \mathbf{\Phi} &= \mathbf{0}. \end{aligned} \tag{5}$$

It is well-known that the DAEs (5) have differentiation index three [16]. The constrained dynamical system can alternatively be described in the Hamiltonian framework. To obtain the corresponding Hamiltonian $H : T^*Q \to \mathbb{R}$, a Legendre transformation can be applied to change the variables $(\mathbf{q}, \dot{\mathbf{q}}) \to (\mathbf{q}, \mathbf{p})$, where the conjugate momentum $\mathbf{p} \in \mathbb{R}^n$ is defined by $\mathbf{p} = \nabla_{\dot{\mathbf{q}}} L$. This leads to

$$H(\mathbf{q}, \mathbf{p}) = \mathbf{p} \cdot \dot{\mathbf{q}} - L(\mathbf{q}, \dot{\mathbf{q}}). \tag{6}$$

For mechanical systems the Hamiltonian is given as the sum of the kinetic energy and the potential energy, i.e. $H(\mathbf{q}, \mathbf{p}) = T(\mathbf{q}, \mathbf{p}) + V(\mathbf{q})$. Similarly to the augmented Lagrangian $L_{\boldsymbol{\gamma}}$, we introduce the augmented Hamiltonian

$$H_{\boldsymbol{\gamma}}(\mathbf{q}, \mathbf{p}) = H(\mathbf{q}, \mathbf{p}) + \boldsymbol{\gamma} \cdot \mathbf{\Phi}(\mathbf{q}). \tag{7}$$

The equations of motion of the constrained mechanical system can now be written in the Hamiltonian framework as

$$\begin{aligned}\dot{\mathbf{q}} &= \nabla_{\mathbf{p}} H(\mathbf{q}, \mathbf{p}) \\ \dot{\mathbf{p}} &= -\nabla_{\mathbf{q}} H(\mathbf{q}, \mathbf{p}) - \nabla_{\mathbf{q}} \boldsymbol{\Phi}^T \boldsymbol{\gamma} \\ \mathbf{0} &= \boldsymbol{\Phi}(\mathbf{q}).\end{aligned} \tag{8}$$

The DAEs (8) are again of differentiation index three. The constraint function on velocity level $\boldsymbol{\Psi}(\mathbf{q}, \dot{\mathbf{q}})$ can now be recast in the form $\boldsymbol{\Psi}(\mathbf{q}, \mathbf{p})$. The index of the DAEs (8) can be reduced to the value of two by appending the constraints on velocity level in the spirit of the GGL method [13, 14]. Accordingly, in the Hamiltonian framework this can be accomplished by introducing the augmented Hamiltonian

$$\tilde{H}_{\boldsymbol{\lambda}}(\mathbf{z}) = H(\mathbf{z}) + \boldsymbol{\lambda} \cdot \boldsymbol{\Theta}(\mathbf{z}), \tag{9}$$

where the phase space coordinates have been collected in

$$\mathbf{z} = \begin{bmatrix} \mathbf{q} \\ \mathbf{p} \end{bmatrix}. \tag{10}$$

Furthermore, both the constraints on configuration level and on velocity level have been arranged in the extended constraint function

$$\boldsymbol{\Theta} = \begin{bmatrix} \boldsymbol{\Phi} \\ \boldsymbol{\Psi} \end{bmatrix} \in \mathbb{R}^{2m}, \tag{11}$$

with corresponding Lagrange multipliers

$$\boldsymbol{\lambda} = \begin{bmatrix} \boldsymbol{\gamma} \\ \boldsymbol{\mu} \end{bmatrix} \in \mathbb{R}^{2m}. \tag{12}$$

Now, the index-2 DAEs can be written in the compact form

$$\begin{aligned}\dot{\mathbf{z}} &= \mathbb{J}\left[\nabla_{\mathbf{z}} H + \nabla_{\mathbf{z}} \boldsymbol{\Theta}^T \boldsymbol{\lambda}\right] \\ \mathbf{0} &= \boldsymbol{\Theta},\end{aligned} \tag{13}$$

where $\mathbb{J}$ is the constant symplectic matrix. Note that on the continuous level the DAEs (13) are equivalent to those in (8). For more details on the DAEs (13) we refer to [5, 14].

3 Galerkin methods in time

In this section we address two alternative Galerkin methods based on the DAEs (13). Both alternative Galerkin methods are implemented in the framework of the finite element method.

3.1 Petrov-Galerkin method

We start with the Petrov-Galerkin method that yields the so-called mixed Galerkin method $mG(k)$, which has originally been introduced in [5]. Applying standard procedures we convert the DAEs (13) into a corresponding weak form. Accordingly, introducing sufficiently

smooth test functions $\delta\mathbf{z}$ and $\delta\boldsymbol{\lambda}$ we obtain

$$\begin{aligned}\int_{t_0}^{t_f} \delta\mathbf{z}\cdot\mathbb{J}^T\left(\dot{\mathbf{z}}-\mathbb{J}\left[\nabla_{\mathbf{z}}H+\nabla_{\mathbf{z}}\boldsymbol{\Theta}^T\boldsymbol{\lambda}\right]\right)\mathrm{d}t=0\\ \int_{t_0}^{t_f} \delta\boldsymbol{\lambda}\cdot\nabla_{\mathbf{z}}\boldsymbol{\Theta}\dot{\mathbf{z}}\,\mathrm{d}t=0,\end{aligned} \tag{14}$$

where the integration is performed over the time interval of interest $\mathcal{T}=[t_0,t_f]$. To obtain a finite element formulation, $\mathcal{T}$ is partitioned into a number of e finite elements

$$\int_{t_0}^{t_f}(\bullet)\,\mathrm{d}t=\sum_{n=1}^{e}\int_{t_{n-1}}^{t_n}(\bullet)\,\mathrm{d}t. \tag{15}$$

The $mG(k)$ method is based on globally continuous approximations for the trial functions

$$\mathbf{z}_h(t)|_{[t_{n-1},t_n]}\in\mathcal{P}^k\left[t_{n-1},t_n\right]^{2n}, \tag{16}$$

where $\mathcal{P}^k[t_{n-1},t_n]$ denotes the set of polynomials of degree k on the interval $[t_{n-1},t_n]$. In contrast to that, the test functions are approximated by globally discontinuous functions

$$\delta\mathbf{z}_h(t)|_{(t_{n-1},t_n)}\in\mathcal{P}^{k-1}\left(t_{n-1},t_n\right)^{2n}. \tag{17}$$

Similarly, the approximations of both the trial functions and the test functions of the Lagrange multipliers are chosen globally discontinuous according to

$$\boldsymbol{\lambda}_h(t),\,\delta\boldsymbol{\lambda}_h(t)|_{(t_{n-1},t_n)}\in\mathcal{P}^{k-1}\left(t_{n-1},t_n\right)^{2m}. \tag{18}$$

For each time finite element on $[t_{n-1},t_n]$ we make use of the coordinate transformation

$$\xi(t)=\frac{t-t_{n-1}}{h_n}, \tag{19}$$

where $h_n=t_{n-1}-t_n$. Correspondingly, the reference element has domain $[0,1]$. The polynomial approximation for each time finite element is based on Lagrangian shape functions

$$N_I(\xi)=\prod_{\substack{J=1\\J\neq I}}^{k+1}\frac{\xi-\xi_J}{\xi_I-\xi_J} \tag{20}$$

where $\xi\in[0,1]$ is the coordinate of the reference element. This leads to the ansatz functions presented in Table 1, enabling the approximations to be written as follows

$$\mathbf{z}_h(\xi)=\sum_{I=1}^{k+1}N_I(\xi)\,\mathbf{z}_I \qquad \delta\mathbf{z}_h(\xi)=\sum_{I=1}^{k}\tilde{N}_I(\xi)\,\delta\mathbf{z}_I \tag{21}$$

$$\boldsymbol{\lambda}_h(\xi)=\sum_{I=1}^{k}\tilde{N}_I(\xi)\,\boldsymbol{\lambda}_I \qquad \delta\boldsymbol{\lambda}_h(\xi)=\sum_{I=1}^{k}\tilde{N}_I(\xi)\,\delta\boldsymbol{\lambda}_I, \tag{22}$$

Table 1 Lagrangian shape functions $N_I(\xi)$

	$k=1$	$k=2$	$k=3$
$N_I(\xi)$	$N_1 = 1-\xi$	$N_1 = (2\xi-1)(\xi-1)$	$N_1 = -\frac{9}{2}(\xi-\frac{1}{3})(\xi-\frac{2}{3})(\xi-1)$
	$N_2 = \xi$	$N_2 = -4(\xi^2-\xi)$	$N_2 = \frac{27}{2}(\xi-\frac{2}{3})(\xi-1)\xi$
		$N_3 = (2\xi-1)\xi$	$N_3 = -\frac{27}{2}(\xi-\frac{1}{3})(\xi-1)\xi$
			$N_4 = \frac{9}{2}(\xi-\frac{1}{3})(\xi-\frac{2}{3})\xi$

where $\tilde{N}_I$ are shape functions one polynomial degree lower than that of N_I. Moreover, the time derivative of $\mathbf{z}_h$ required in (14) is given by

$$\dot{\mathbf{z}}_h(\xi) = \sum_{I=1}^{k+1} h_n^{-1} N_I'(\xi)\, \mathbf{z}_I. \tag{23}$$

Due to the discontinuous test functions in the $mG(k)$ method, the algebraic equations for each time finite element are decoupled from the other time finite elements. Accordingly, the unknown nodal values $\mathbf{z}_I$ and $\boldsymbol{\lambda}_I$ can be determined individually for each element. This way the usual time-stepping format is recovered and the solution of the initial value problem can be achieved by marching forward in time with the time-step size h_n. Note that due to the continuity of the discrete trial functions, the nodal values $\mathbf{z}_1$ are given for each element.

We further remark that in the weak form $(14)_2$, the original constraint equation $(13)_2$ has been differentiated once with respect to time. This feature of the $mG(k)$ method ensures algorithmic energy conservation (see [5] for further details). Moreover, if the holonomic constraints are at most quadratic, the $mG(k)$ method enforces satisfaction of the algebraic constraints at the end-point of each time step. That is, $\boldsymbol{\Theta}(\mathbf{z}_{n+1}) = \mathbf{0}$, provided that $\boldsymbol{\Theta}(\mathbf{z}_n) = \mathbf{0}$ holds (cf. Sect. 2.3.1 in [5]). For higher nonlinearity of the holonomic constraints, the derivative of the constraints can be replaced with an appropriately constructed discrete derivative to retain the fulfillment of the constraints at the end of the time step.

3.2 Bubnov-Galerkin method

Similarly to the Petrov-Galerkin method dealt with in Sect. 3.1, the Bubnov-Galerkin method hinges on the weak form of the equations of motion (13) given by

$$\begin{aligned} &\int_{t_0}^{t_f} \delta\mathbf{z} \cdot \mathbb{J}^T \left(\dot{\mathbf{z}} - \mathbb{J}\left[\nabla_{\mathbf{z}} H + \nabla_{\mathbf{z}} \boldsymbol{\Theta}^T \boldsymbol{\lambda}\right]\right) \mathrm{d}t = 0 \\ &\int_{t_0}^{t_f} \delta\boldsymbol{\lambda} \cdot \boldsymbol{\Theta}\, \mathrm{d}t = 0. \end{aligned} \tag{24}$$

The Bubnov-Galerkin method uses the same function spaces for the test and trial functions. In particular, for each time finite element we introduce globally continuous approximating polynomials

$$\mathbf{z}_h(t), \delta\mathbf{z}_h(t)|_{[t_{n-1},t_n]} \in \mathcal{P}^k\left[t_{n-1}, t_n\right]^{2n}, \tag{25}$$

where, as before, $\mathcal{P}^k[t_{n-1}, t_n]$ denotes the set of polynomials of degree k on the interval $[t_{n-1}, t_n]$. Concerning the approximation of the Lagrange multipliers, we may use either globally continuous or discontinuous piecewise interpolations. Accordingly, we either

choose

$$\boldsymbol{\lambda}_h(t), \delta\boldsymbol{\lambda}_h(t)|_{[t_{n-1},t_n]} \in \mathcal{P}^k\left[t_{n-1}, t_n\right]^{2m}, \tag{26}$$

or

$$\boldsymbol{\lambda}_h(t), \delta\boldsymbol{\lambda}_h(t)|_{(t_{n-1},t_n)} \in \mathcal{P}^{k-1}\left(t_{n-1}, t_n\right)^{2m}. \tag{27}$$

For each time finite element the shape functions introduced in the last section can be used to realize the finite element implementation of the present Bubnov-Galerkin method. The main difference from the previous Petrov-Galerkin method is the global continuity of the test functions in (25) and (26). Thus, the element contributions must be assembled, resulting in a global system of algebraic equations corresponding to the entire time interval of interest $\mathcal{T} = [t_0, t_f]$. Accordingly, we no longer have a time-stepping scheme. However, the global solution procedure can still be partitioned, leading to a block-wise solution procedure (see [11]).

The system of nonlinear algebraic equations emanating from both the Bubnov-Galerkin method and the Petrov-Galerkin method can be solved iteratively by applying Newton's method.

4 Rigid bodies as constrained mechanical systems

As outlined in Sect. 1, rigid bodies can be regarded as constrained mechanical systems by using redundant coordinates for the parametrization of their motion. Accordingly, in what follows, we describe rigid body dynamics in terms of unit quaternions and director triads.

4.1 Kinematics

Consider a rigid body in the reference configuration $\mathcal{B}_0$ with mass density ρ_0 and an orthonormal basis $\{\mathbf{e}_1, \mathbf{e}_2, \mathbf{e}_3\}$ fixed in the center of mass of $\mathcal{B}_0$ (Fig. 1). For simplicity we assume that the base vectors $\mathbf{e}_i$ are aligned with the principal axes of the rigid body. The motion of the rigid body can be described by the deformation map, which maps material points $\mathbf{X} = X_i\mathbf{e}_i$ (the summation convention applies to repeated indices) in $\mathcal{B}_0$ to their placement in the current configuration $\mathcal{B}$ at time t via

$$\mathbf{x}(\mathbf{X}, t) = \boldsymbol{\varphi}(t) + \mathbf{R}(t)\mathbf{X}. \tag{28}$$

Here, $\boldsymbol{\varphi}(t)$ denotes the position vector of the center of mass and $\mathbf{R}(t) \in SO(3)$ is the rotation matrix $\mathbf{R} \in SO(3)$, which characterizes the orientation of the body-fixed orthonormal frame $\{\mathbf{d}_1, \mathbf{d}_2, \mathbf{d}_3\}$ such that $\mathbf{d}_i = \mathbf{R}\mathbf{e}_i$. Note that $\mathbf{R}(0) = \mathbf{I}$ and $\boldsymbol{\varphi}(0) = \mathbf{0}$, so that $\mathbf{x}(\mathbf{X}, 0) = \mathbf{X}$. The material velocity $\dot{\mathbf{x}} = \frac{\partial \mathbf{x}}{\partial t}$ takes the form

$$\dot{\mathbf{x}}(\mathbf{X}, t) = \dot{\boldsymbol{\varphi}}(t) + \dot{\mathbf{R}}(t)\mathbf{X}, \tag{29}$$

where $\dot{\mathbf{R}} \in T_{\mathbf{R}}SO(3)$ belongs to the tangent space of the rotational configuration space

$$\dot{\mathbf{R}} = \mathbf{R}\hat{\boldsymbol{\Omega}}, \tag{30}$$

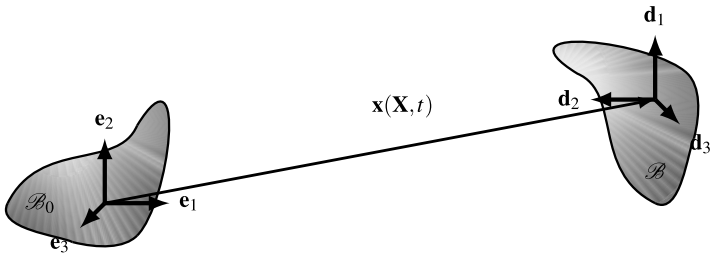

Fig. 1 Rigid Body configurations $\mathcal{B}_0$ and $\mathcal{B}$

with the skew-symmetric matrix $\hat{\mathbf{\Omega}} \in \mathbb{R}^{3\times 3}$, which follows from the differentiation of the orthogonality condition $\mathbf{R}^T\mathbf{R} = \mathbf{I}$ with respect to time, see [24]. The skew-symmetric matrix $\hat{\mathbf{\Omega}}$ can be related to the convective angular velocity vector $\mathbf{\Omega} \in \mathbb{R}^3$ via

$$\hat{\mathbf{\Omega}}\mathbf{a} = \mathbf{\Omega} \times \mathbf{a}, \tag{31}$$

where $\mathbf{a} \in \mathbb{R}^3$ is an arbitrary vector. The kinetic energy of the rigid body is defined by

$$T = \int_{\mathcal{B}_0} \frac{1}{2}\rho_0(\mathbf{X})\dot{\mathbf{x}} \cdot \dot{\mathbf{x}}\, \mathrm{d}V. \tag{32}$$

Substituting (29) into the last equation, we obtain

$$T = \frac{1}{2} M_\varphi \dot{\boldsymbol{\varphi}} \cdot \dot{\boldsymbol{\varphi}} + T_{rot}, \tag{33}$$

where the rotational part of the kinetic energy relative to the center of mass is given by

$$T_{rot} = \frac{1}{2}\mathbf{\Omega} \cdot \mathbf{J}\mathbf{\Omega}, \tag{34}$$

with the convected inertia tensor

$$\mathbf{J} = \int_{\mathcal{B}_0} \rho_0(\mathbf{X}) \left(|\mathbf{X}|^2 \mathbf{I} - \mathbf{X} \otimes \mathbf{X} \right) \mathrm{d}\mathcal{B}_0. \tag{35}$$

4.2 Unit quaternions

A quaternion can be considered as a tuple of real numbers

$$\mathfrak{q} = [q_0, \mathbf{q}] \in \mathbb{H} \simeq \mathbb{R}^4, \tag{36}$$

where $q_0 \in \mathbb{R}$ is the scalar part and $\mathbf{q} \in \mathbb{R}^3$ is the vector part, which can be written as $\mathbf{q} = q_i \mathbf{e}_i$ where $\mathbf{e}_i, i = 1, 2, 3$ is the standard orthonormal basis in $\mathbb{R}^3$. The non-commutative quaternion product of $\mathfrak{q}$ and $\mathfrak{p}$ is defined by

$$\mathfrak{q} \circ \mathfrak{p} = [q_0 p_0 - \mathbf{q} \cdot \mathbf{p}, q_0\mathbf{p} + p_0\mathbf{q} + \mathbf{q} \times \mathbf{p}], \tag{37}$$

where $(\bullet) \cdot (\bullet)$ denotes the standard scalar product and $(\bullet) \times (\bullet)$ the vector cross product. Consequently, the norm of a quaternion is defined as follows

$$|\mathbb{q}| = \sqrt{q_0^2 + q_1^2 + q_2^2 + q_3^2}. \tag{38}$$

The conjugate $\overline{\mathbb{q}}$ of a quaternion $\mathbb{q}$ is expressed as

$$\overline{\mathbb{q}} = [q_0, -\mathbf{q}]. \tag{39}$$

The inverse of a quaternion is given by

$$\mathbb{q}^{-1} = \frac{1}{|\mathbb{q}|^2} \overline{\mathbb{q}}. \tag{40}$$

Note that each unique rotation can be represented by $\mathbb{q}$ and its antipodal counterpart $-\mathbb{q}$.

For further rules on handling quaternions and a detailed algebraic overview we refer to [1]. Pure quaternions are a subset $\mathbb{H}_0$, where the scalar part q_0 is zero. An important subset of quaternions are unit quaternions $\mathbb{q} = [q_0, \mathbf{q}] \in \mathbb{H}_1$, whose norm is restricted to the unit norm $|\mathbb{q}| = 1$ [8]. The set $\mathbb{H}_1$ corresponds to the hypersurface S^3 in the quaternion space, which concurrently represents the unit sphere in $\mathbb{R}^4$ [24]

$$S^3 = \left\{ \mathbb{q} \in \mathbb{R}^4 : |\mathbb{q}| = 1 \right\}. \tag{41}$$

4.2.1 Matrix representation of quaternions

For easy handling of the quaternions, it is preferable to use them in a matrix representation, where the quaternions are regarded as a column matrix $\mathbb{q} \in \mathbb{H} \simeq \mathbb{R}^4$. For further information about the matrix representation we refer to [2] and the references cited therein. The quaternion multiplication (37) can be written in the matrix representation

$$\mathbb{q} \circ \mathbb{p} = \mathbf{Q}_l(\mathbb{q})\, \mathbb{p} = \mathbf{Q}_r(\mathbb{p})\, \mathbb{q}, \tag{42}$$

where $\mathbf{Q}_l, \mathbf{Q}_r \in \mathbb{R}^{4\times4}$ is defined by

$$\begin{aligned} \mathbf{Q}_l(\mathbb{q}) &= \begin{bmatrix} \mathbb{q} & \mathbf{G}(\mathbb{q})^T \end{bmatrix} \\ \mathbf{Q}_r(\mathbb{q}) &= \begin{bmatrix} \mathbb{q} & \mathbf{E}(\mathbb{q})^T \end{bmatrix}. \end{aligned} \tag{43}$$

The non-square matrices

$$\begin{aligned} \mathbf{G}(\mathbb{q}) &= \begin{bmatrix} -\mathbf{q} & q_0 \mathbf{I}_3 - \hat{\mathbf{q}} \end{bmatrix} \\ \mathbf{E}(\mathbb{q}) &= \begin{bmatrix} -\mathbf{q} & q_0 \mathbf{I}_3 + \hat{\mathbf{q}} \end{bmatrix} \end{aligned} \tag{44}$$

are characterized by the skew-symmetric matrix $\hat{\mathbf{q}} \in \mathbb{R}^{3\times3}$

$$\hat{\mathbf{q}} = \begin{bmatrix} 0 & -q_3 & q_2 \\ q_3 & 0 & -q_1 \\ -q_2 & q_1 & 0 \end{bmatrix}. \tag{45}$$

Orthogonality of $\mathbf{Q}_l$ and $\mathbf{Q}_r$ applies in particular to unit quaternions

$$\begin{aligned} \mathbf{Q}_l(\mathfrak{q})^{-1} &= \mathbf{Q}_l(\mathfrak{q})^T \\ \mathbf{Q}_r(\mathfrak{q})^{-1} &= \mathbf{Q}_r(\mathfrak{q})^T. \end{aligned} \tag{46}$$

Moreover the following equations hold for unit quaternions

$$\begin{aligned} \mathbf{Q}_l(\mathfrak{q})^T &= \mathbf{Q}_l(\overline{\mathfrak{q}}) \\ \mathbf{Q}_r(\mathfrak{q})^T &= \mathbf{Q}_r(\overline{\mathfrak{q}}). \end{aligned} \tag{47}$$

To obtain the rotational energy in quaternion formulation we have to describe the convective angular velocity $\boldsymbol{\Omega}$ in terms of the unit quaternions. Therefor we have to consider the tangential space of the unit quaternions $T_{\mathfrak{q}}S^3$, which can be obtained by differentiating the unit length constraint with respect to time

$$\dot{\overline{\mathfrak{q}}} \circ \mathfrak{q} + \overline{\mathfrak{q}} \circ \dot{\mathfrak{q}} = [0, \mathbf{0}]. \tag{48}$$

This indicates the relationship with the convective angular velocity

$$\overline{\mathfrak{q}} \circ \dot{\mathfrak{q}} = \left[0, \tfrac{1}{2}\boldsymbol{\Omega}\right], \tag{49}$$

where the angular velocity is introduced as a pure quaternion

$$\mathfrak{\Omega} = \begin{bmatrix} 0 \\ \boldsymbol{\Omega} \end{bmatrix} \in \mathbb{H}_0. \tag{50}$$

Employing matrix representation (42), the angular velocities can be written as

$$\begin{aligned} \mathfrak{\Omega} &= 2\mathbf{Q}_l(\mathfrak{q})^T \dot{\mathfrak{q}} \\ \mathfrak{w} &= 2\mathbf{Q}_r(\mathfrak{q})^T \dot{\mathfrak{q}}, \end{aligned} \tag{51}$$

or

$$\begin{aligned} \boldsymbol{\Omega} &= 2\mathbf{G}(\mathfrak{q})\dot{\mathfrak{q}} \\ \boldsymbol{\omega} &= 2\mathbf{E}(\mathfrak{q})\dot{\mathfrak{q}}, \end{aligned} \tag{52}$$

where $\boldsymbol{\omega} \in \mathbb{R}^3$ denotes the spatial angular velocity and $\mathfrak{w} \in \mathbb{H}_0$ the corresponding pure quaternion form. In the Hamilton framework the mass matrix must be invertible, which is possible by using (51). Unlike $\mathbf{G}(\mathfrak{q})$ the matrices $\mathbf{Q}_l(\mathfrak{q})$ are non-singular. The relative rotational kinetic energy in quaternion formulation follows as

$$T_{Rot} = \frac{1}{2}\, \mathfrak{\Omega} \cdot \mathbf{J}_4\, \mathfrak{\Omega}, \tag{53}$$

where that mass matrix is given by

$$\mathbf{J}_4 = \begin{bmatrix} J_0 & \mathbf{0}^T \\ \mathbf{0} & \mathbf{J} \end{bmatrix}. \tag{54}$$

Accordingly, the inertia tensor $\mathbf{J}$ is extended by $J_0 = \frac{1}{2}\text{tr}(\mathbf{J})$, which serves to increase the rank of the mass matrix without affecting the dynamical system, as this extension is eliminated by the multiplication with the pure quaternion. Now, the relative rotational kinetic energy can be written in the form

$$T_{Rot}(\mathbb{q}, \dot{\mathbb{q}}) = 2\dot{\mathbb{q}} \cdot \mathbf{M}_4(\mathbb{q})\dot{\mathbb{q}}, \tag{55}$$

where the extended mass matrix is given by

$$\mathbf{M}_4(\mathbb{q}) = \mathbf{Q}_l(\mathbb{q})\mathbf{J}_4\mathbf{Q}_l(\mathbb{q})^T. \tag{56}$$

The conjugate momentum can be calculated as

$$\mathbb{p} = 4\mathbf{M}_4(\mathbb{q})\dot{\mathbb{q}} \tag{57}$$

leading to the following expression for the relative rotational kinetic energy

$$T_{Rot}(\mathbb{q}, \mathbb{p}) = \frac{1}{8}\,\mathbb{p} \cdot \mathbf{M}_4(\mathbb{q})^{-1}\,\mathbb{p}\,. \tag{58}$$

The total kinetic energy (33) now enters the augmented Hamiltonian (7). In this connection, the unit-length constraint on the quaternion yields the constraint function

$$\Phi(\mathbb{q}) = \frac{1}{2}\,(\mathbb{q} \cdot \mathbb{q} - 1)\,. \tag{59}$$

The resulting equations of motion in terms of unit quaternions are provided in the Appendix.

4.3 Director formulation

The rotational motion of the rigid body can also be described directly in terms of the director triad [4]. Accordingly, the rotation of the rigid body can be described by body-fixed director triad $\{\mathbf{d}_1, \mathbf{d}_2, \mathbf{d}_3\}$, which results in

$$\mathbf{R} = \mathbf{d}_i \otimes \mathbf{e}_i\,. \tag{60}$$

Using this representation of the rotation matrix, the material velocity (29) can be written as

$$\dot{\mathbf{x}}(\mathbf{X}, t) = \dot{\boldsymbol{\varphi}}(t) + \dot{\mathbf{d}}_k X_k, \tag{61}$$

where we recall that the summation over $k = 1, 2, 3$ applies according to the summation convention. Substituting (61) into the kinetic energy of the rigid body (32) we obtain the following quadratic form

$$T = \frac{1}{2}\dot{\mathbf{q}} \cdot \mathbf{M}\dot{\mathbf{q}}, \tag{62}$$

where

$$\dot{\mathbf{q}} = \begin{bmatrix} \dot{\boldsymbol{\varphi}} \\ \dot{\mathbf{d}}_1 \\ \dot{\mathbf{d}}_2 \\ \dot{\mathbf{d}}_3 \end{bmatrix} \qquad \mathbf{M} = \begin{bmatrix} M_\varphi \mathbf{I} & S_1\mathbf{I} & S_2\mathbf{I} & S_3\mathbf{I} \\ & E_{11}\mathbf{I} & E_{12}\mathbf{I} & E_{13}\mathbf{I} \\ & & E_{22}\mathbf{I} & E_{23}\mathbf{I} \\ & & & E_{33}\mathbf{I} \end{bmatrix} \tag{63}$$

and

$$M_\varphi = \int_{\mathcal{B}_0} \rho_0 \, \mathrm{d}V, \quad S_k = \int_{\mathcal{B}_0} \rho_0 X_k \, \mathrm{d}V, \quad E_{ik} = \int_{\mathcal{B}_0} \rho_0 X_i X_k \, \mathrm{d}V. \tag{64}$$

Note that by the assumption that the reference frame is placed in the center of mass, $S_k = 0$ holds. The mass matrix further simplifies to diagonal form due to the assumption of principal axes. We further note that the convected inertia tensor $\mathbf{J}$ can be linked to the convected Euler tensor $\mathbf{E} = E_{ik}\mathbf{e}_i \otimes \mathbf{e}_k$ through the relation $\mathbf{J} = \mathrm{tr}(\mathbf{E})\mathbf{I} - \mathbf{E}$, for more details see [4].

The total kinetic energy (62) now enters the augmented Hamiltonian (7). In this connection, there are six independent constraints of orthonormality on the director triad leading to the constraint function

$$\boldsymbol{\Phi}(\mathbf{q}) = \begin{bmatrix} \frac{1}{2}(\mathbf{d}_1 \cdot \mathbf{d}_1 - 1) \\ \frac{1}{2}(\mathbf{d}_2 \cdot \mathbf{d}_2 - 1) \\ \frac{1}{2}(\mathbf{d}_3 \cdot \mathbf{d}_3 - 1) \\ \mathbf{d}_1 \cdot \mathbf{d}_2 \\ \mathbf{d}_1 \cdot \mathbf{d}_3 \\ \mathbf{d}_2 \cdot \mathbf{d}_3 \end{bmatrix}. \tag{65}$$

5 Numerical investigation

5.1 Spinning box

This example has been taken from [20]. Accordingly, we consider a cuboid with dimensions $l = 5$, $b = 2$, $h = 1$ and a constant mass density leading to the total mass $m = 12$. The origin of the reference frame coincides with the center of mass and the coordinate axes are aligned with the principal axes of the body. The initial conditions are $\mathfrak{q}_0 = [1\ 0\ 0\ 0]^T$ (or $\mathbf{R}_0 = \mathbf{I}$) and $\boldsymbol{\Omega}_0 = [0\ 5\ 1]^T$.

The cuboid can spin freely in space. Snapshots of the motion are shown in Fig. 2. Both the total energy and the total angular momentum of the body are conserved quantities.

The algorithmic conservation properties of the $mG(k)$ method for both the director formulation and the quaternion formulation are depicted in Figs. 3 and 4. In the director formulation, the $mG(k)$ method preserves both angular momentum and energy, as proven in [4] and corroborated in Fig. 3.

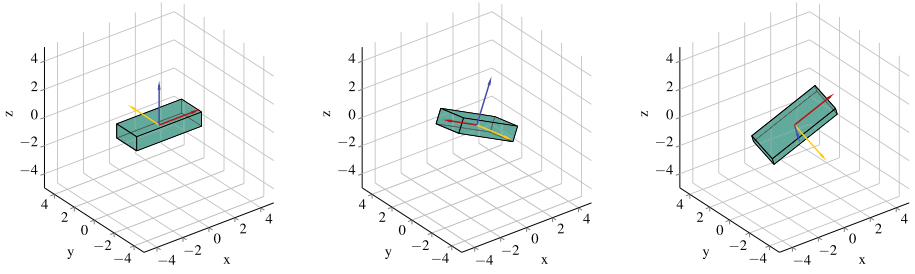

Fig. 2 Snapshots of the rotating cuboid (obtained with $mG(3)$ with $h_n = 0.05$)

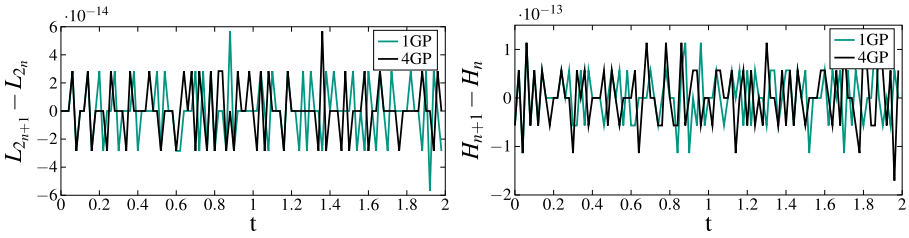

Fig. 3 Conservation of angular momentum L_2 (left) and energy (right) for the $mG(1)$ method in the director formulation for different Gauss points (GP), $h_n = 0.05$

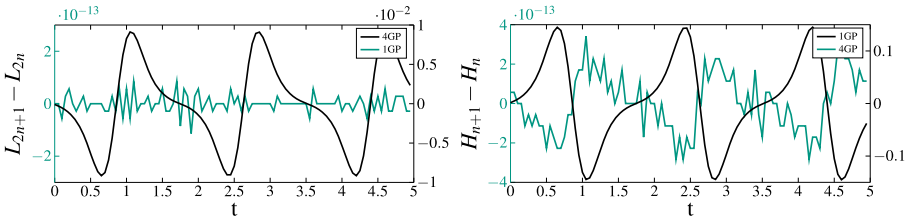

Fig. 4 Conservation of angular momentum L_2 (left) and energy (right) for the $mG(1)$ method in the quaternion formulation for different Gauss points (GP), $h_n = 0.05$

However, in the quaternion formulation, the algorithmic conservation properties of the $mG(k)$ method depend on the choice of the Gaussian quadrature formula for evaluating the time integrals in the element formulation. Figure 4 illustrates how algorithmic conservation of the total angular momentum component L_2 (left) and the total Hamiltonian (right) are affected by the number of Gauss points. While angular momentum remains conserved with just one Gauss point (placed at the center of the element), energy conservation requires four Gauss points. This observation aligns with the requirements of the Petrov-Galerkin formulation described in [3]. Evidently, the quaternion formulation of the $mG(k)$ method does not allow the simultaneous conservation of both quantities when using standard Gaussian quadrature. Indeed, the method in [2] can be regarded as energy-momentum consistent modification of the $mG(k)$ method.

The conservation properties of the global Bubnov-Galerkin approach based on the quaternion formulation are shown in Fig. 5, exemplarily for cubic ansatz functions and a discontinuous approximation of the Lagrange multipliers. It can be observed that the global

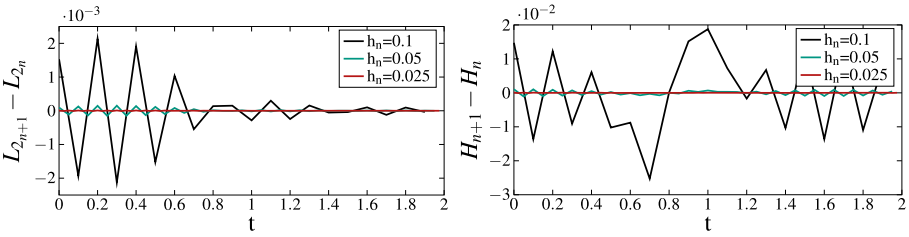

Fig. 5 Conservation of angular momentum L_2 (left) and energy (right) for the Bubnov-Galerkin method ($k = 3$) based on the quaternion formulation for different time steps sizes

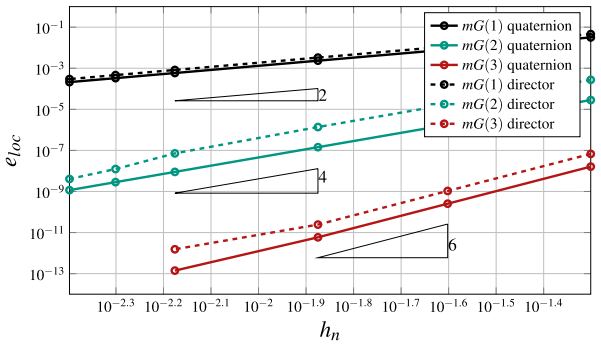

Fig. 6 Convergence of $mG(k)$ method for both the quaternion and director formulations

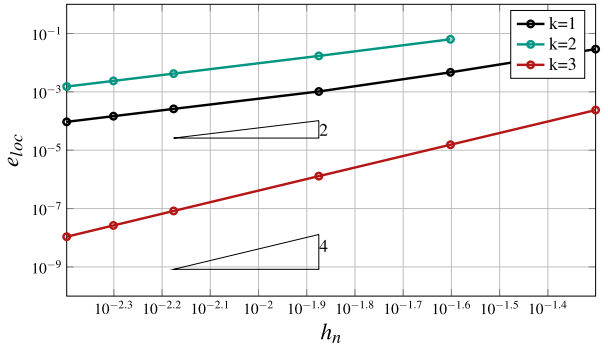

Fig. 7 Convergence of the global Bubnov-Galerkin method in the quaternion-based formulation for different polynomial degrees k

Bubnov-Galerkin method neither conserves total angular momentum nor total energy algorithmically. However, as the time step decreases, algorithmic conservation properties do improve.

We next examine the numerical error at the end point $t_f = 5$. For this, we define a local configuration error

$$e_{loc} = \frac{||\mathbf{q}_{Ref}(t_f) - \mathbf{q}^h(t_f)||}{||\mathbf{q}_{Ref}(t_f)||}, \tag{66}$$

where $\mathbf{q}_{Ref}(t_f)$ is the reference solution which is calculated with $mG(3)$, 50,000 cubic time elements and a Newton tolerance of $\varepsilon = 10^{-12}$. Figure 6 shows the convergence behavior of the $mG(k)$ method for both rigid body formulations under investigation and different ansatz functions. The results show that the local error decreases as $e_{loc} = \mathcal{O}(h_n^{2k})$ for both rigid body formulations.

Similarly, Fig. 7 depicts the convergence of the global Bubnov-Galerkin method for the quaternion-based formulation and different polynomial degrees k. It can be observed that all schemes converge despite the fact that increasing the polynomial degree k does not show an improvement of accuracy comparable to the $mG(k)$ method. The results remain nearly unchanged regardless of whether the Lagrange multipliers are approximated continuously or discontinuously. Moreover, both the quaternion-based and the director-based formulations essentially yield the same convergence results.

Figure 8 shows the condition number of the assembled tangent matrix (iteration matrix in Newton's method) depending on the size of the time step for the global Bubnov-Galerkin

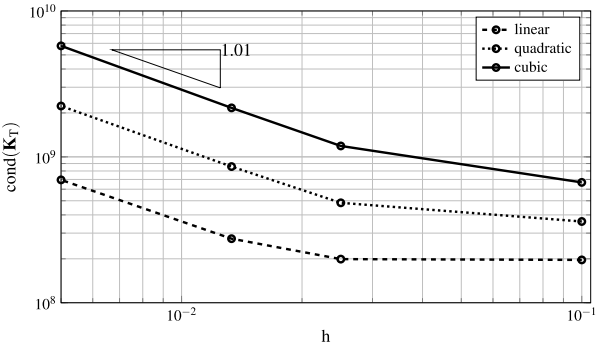

Fig. 8 Condition number of the iteration matrix plotted over the time step size of the Bubnov-Galerkin method applied to the quaternion formulation

method, in which the Lagrange multipliers are continuously approximated. It can be seen that the condition number grows only with $O(h_n^1)$. In contrast to that, the condition number of the iteration matrix pertaining to the $mG(k)$ method grows with $O(h_n^2)$, since the underlying DAEs have index two. Note however, that scaling techniques can be applied to improve the conditioning of directly integrated DAEs [6].

5.2 Physical pendulum

In contrast to the mass point of the mathematical pendulum, the physical pendulum contains a rigid body that rotates about a fixed support point. As in the first example, the rigid body is a cuboid with dimensions $l = 10$, $b = h = 1$ and a constant mass density $\rho_0 = 10$. Note that in this case, besides enforcing the internal constraint of rigidity (unit-length condition in the quaternion-based formulation), we also need to impose an external constraint $\mathbf{\Phi}^e$ to ensure rotation about the support point. In particular, the additional external constraint is given by

$$\mathbf{\Phi}^e(\mathbb{q}) = \mathbf{R}(\mathbb{q})\boldsymbol{\varphi}_0 - \boldsymbol{\varphi}. \tag{67}$$

Moreover, gravity is acting on the pendulum leading to the potential $V(\mathbf{q}) = M_\varphi \boldsymbol{\varphi} \cdot \mathbf{g}$, where the gravitational acceleration is given by $\mathbf{g} = [0\ 0\ 9.81]^T$. The initial configuration is given by $\boldsymbol{\varphi}_0 = [0\ l/2\ 0]^T$, $\mathbb{q}_0 = [1\ 0\ 0\ 0]^T$ and the initial velocity is assumed to be zero. The motion of the physical pendulum is illustrated in Fig. 9, which shows snapshots of the initial configuration ($t = 0$) of the pendulum and configurations at selected later time points.

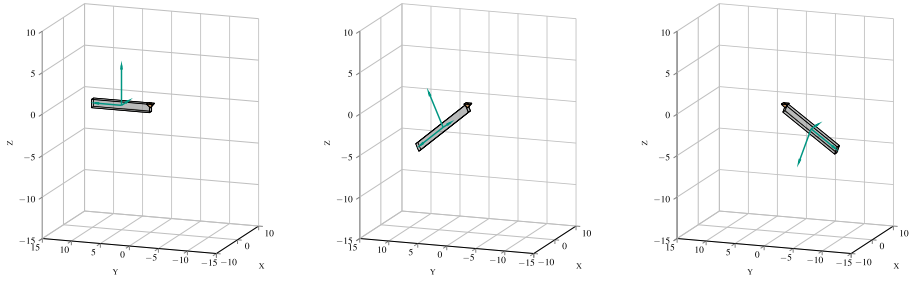

$t = 0$ $t = 7$ $t = 10$

Fig. 9 Snapshots of the physical pendulum obtained with the $mG(1)$ method and $h_n = 0.1$

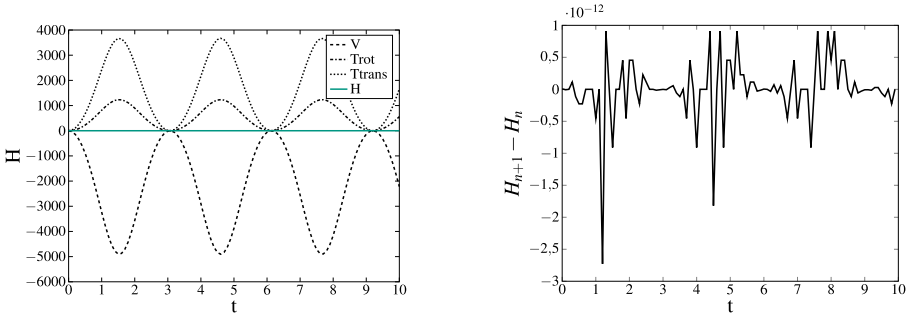

Fig. 10 Conservation of the Hamiltonian obtained with the $mG(1)$ method for the quaternion-based formulation ($4GP$, $h_n = 0.1s$)

Figure 10 confirms that the $mG(k)$ method is capable to conserve the Hamiltonian of the constrained system at hand. Moreover, all of the constraints are satisfied at the end of each time step as illustrated in Fig. 11. The left-hand diagram depicts the internal constraints on configuration and velocity level, which are satisfied exactly up to machine precision, while the right-hand diagram depicts the external constraints, which are also precisely enforced.

Unlike the exact enforcement of the constraints at each node, the global Bubnov-Galerkin method satisfies the constraints in an averaged or integral manner. This behavior is illustrated in Fig. 12 for linear ansatz functions and continuous Lagrange multipliers. It is evident that constraint satisfaction improves as the time step size decreases.

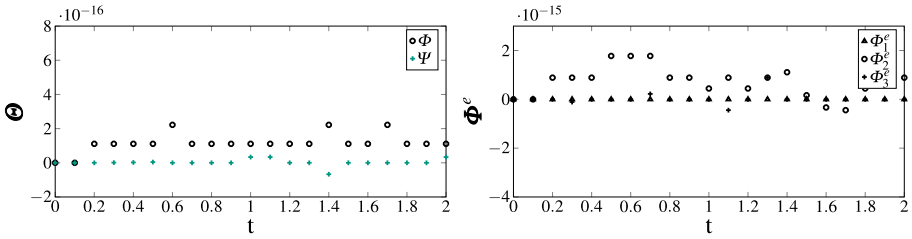

Fig. 11 Internal constraints related to the unit-length condition of the quaternion (left) and components of the external constraints (67) (right), $mG(1)$ method, $h_n = 0.1s$

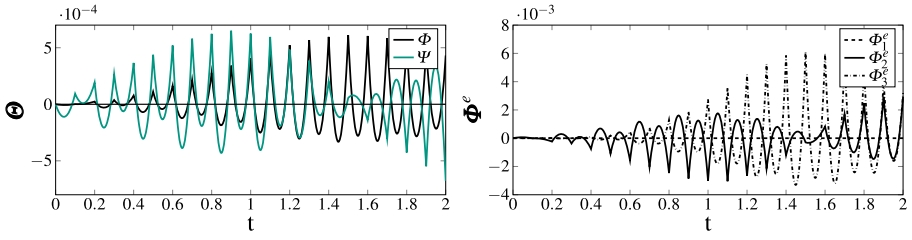

Fig. 12 Internal constraints related to the unit-length condition of the quaternion (left) and components of the external constraints (67) (right), global Bubnov-Galerkin method, $h_n = 0.1s$

6 Conclusions

In the present work Galerkin-based time integration methods have been investigated for discrete mechanical systems subject to holonomic constraints. The Petrov-Galerkin formulation, termed $mG(k)$ method, is based on globally discontinuous test functions and thus recovers the common time-stepping format of numerical schemes for the solution of initial value problems. On the other hand, the Bubnov-Galerkin method relies on globally continuous test functions and thus requires an assembly procedure for the time finite elements spanning the time interval of interest. The global Bubnov-Galerkin approach was originally proposed by [11] in the context of a rigid body formulation based on director triads. In the present work we have newly adopted the global Bubnov-Galerkin method to a rigid body formulation in terms of unit-quaternions. In addition to that, we have applied the $mG(k)$ method, originally developed in [5], to the quaternion-based rigid body formulation for the first time. Moreover, the quaternion-based formulations have been compared to an alternative description of the rotational rigid body motion in terms of director triads. Due to the presence of holonomic constraints, all of the methods under investigation can be easily applied to multibody system dynamics.

In contrast to the $mG(k)$ method based on directors, the alternative formulation in terms of quaternions is not able to algorithmically conserve both the total energy and the total angular momentum at the same time. This is due to the increased nonlinearity of the quaternion-based formulation, which is reflected by a configuration-dependent mass matrix. Moreover, the global Bubnov-Galerkin method does not appear beneficial for the solution of initial value problems, when compared to the common time-stepping format of the $mG(k)$ method. Apart from the significantly increased size of the algebraic system of equations to be solved, the accuracy of the global Bubnov-Galerkin approach turned out to be inferior to that of the $mG(k)$ method. However, the global solution procedure is deemed to be of importance for the solution of inverse dynamics problems and optimal control problems.

Appendix: Strong form of equations of motions

The equations of motion in director formulation results in

$$\begin{aligned} \dot{\mathbf{q}} &= \mathbf{M}^{-1}\mathbf{p} + \nabla_{\mathbf{p}}\boldsymbol{\Psi}^{\mathrm{T}}\boldsymbol{\mu} \\ \dot{\mathbf{p}} &= -\nabla_{\mathbf{q}}V - \nabla_{\mathbf{q}}\boldsymbol{\Phi}^{\mathrm{T}}\boldsymbol{\gamma} - \nabla_{\mathbf{q}}\boldsymbol{\Psi}^{\mathrm{T}}\boldsymbol{\mu} \\ \mathbf{0} &= \boldsymbol{\Theta}. \end{aligned} \tag{68}$$

The quaternion formulation leads to a non-constant mass matrix. Based on the previous kinematic assumptions, this results in the following equations of motion

$$\begin{aligned} \dot{\mathbf{q}} &= \begin{bmatrix} \mathbf{M}_{\varphi}^{-1}\mathbf{p}_{\varphi} \\ \frac{1}{4}\mathbf{M}_4^{-1}(\mathbb{q})\,\mathbb{p} + \mu\nabla_{\mathbb{q}}\Psi \end{bmatrix} = \begin{bmatrix} \dot{\boldsymbol{\varphi}} \\ \dot{\mathbb{q}} \end{bmatrix} \\ \dot{\mathbf{p}} &= \begin{bmatrix} \mathbf{0} \\ -\frac{1}{4}\mathbf{M}_4^{-1}(\mathbb{p})\,\mathbb{q} - \gamma\nabla_{\mathbb{q}}\Phi - \mu\nabla_{\mathbb{q}}\Psi \end{bmatrix} = \begin{bmatrix} \dot{\mathbf{p}}_{\varphi} \\ \dot{\mathbb{p}} \end{bmatrix} \\ \mathbf{0} &= \boldsymbol{\Theta}. \end{aligned} \tag{69}$$

Here, $\mathbf{M}_{\varphi} = M_{\varphi}\mathbf{I}$, where M_{φ} has been introduced in (64) and denotes the total mass of the rigid body. For convenience in calculating the derivatives in the second Hamilton equation,

the rotational energy (58) can be reformulated as follows:

$$T_{Rot}(\mathfrak{q}, \mathfrak{p}) = \frac{1}{8}\, \mathfrak{q}^{\,T} \mathbf{M}_4(\mathfrak{p})^{-1}\, \mathfrak{q}, \tag{70}$$

see [20].

Author contributions MM: Methodology, idea development, implementation, investigation, data curation, writing and editing, visualization. PB: Methodology, idea development, resources, writing–review and editing, supervision, project administration.

Funding information Open Access funding enabled and organized by Projekt DEAL.

Data availability No datasets were generated or analysed during the current study.

Declarations

Competing interests The authors declare no competing interests.

References

1. Altmann, S.L.: Rotations, Quaternions, and Double Groups. Oxford University Press, Oxford (1986)
2. Betsch, P., Siebert, R.: Rigid body dynamics in terms of quaternions: Hamiltonian formulation and conserving numerical integration. Int. J. Numer. Methods Eng. **79**(4), 444–473 (2009). https://doi.org/10.1002/nme.2586
3. Betsch, P., Steinmann, P.: Conservation properties of a time FE method. Part I: time-stepping schemes for n-body problems. Int. J. Numer. Methods Eng. **49**(5), 599–638 (2000). https://doi.org/10.1002/1097-0207(20001020)49:5<599::AID-NME960>3.0.CO;2-9
4. Betsch, P., Steinmann, P.: Constrained integration of rigid body dynamics. Comput. Methods Appl. Mech. Eng. **191**(3), 467–488 (2001). https://doi.org/10.1016/S0045-7825(01)00283-3
5. Betsch, P., Steinmann, P.: Conservation properties of a time FE method-part III: mechanical systems with holonomic constraints. Int. J. Numer. Methods Eng. **53**(10), 2271–2304 (2002). https://doi.org/10.1002/nme.347
6. Bottasso, C.L., Bauchau, O.A., Cardona, A.: Time-step-size-independent conditioning and sensitivity to perturbations in the numerical solution of index three differential algebraic equations. SIAM J. Sci. Comput. **29**(1), 397–414 (2007). https://doi.org/10.1137/050638503
7. Chaturvedi, N.A., Sanyal, A.K., McClamroch, N.H.: Rigid-body attitude control. IEEE Control Syst. Mag. **31**(3), 30–51 (2011). https://doi.org/10.1109/MCS.2011.940459
8. Dam, E.B., Koch, M., Lillholm, M.: Quaternions, interpolation and animation. Tech. Rep. DIKU-TR-98/5, Department of Computer Science, University of Copenhagen (1998)
9. Gerdts, M.: Optimal Control of ODEs and DAEs, 2nd edn. De Gruyter Oldenbourg, Berlin (2024). https://doi.org/10.1515/9783110797893
10. Haug, E.: Computer-Aided Kinematics and Dynamics of Mechanical Systems. Volume I: Basic Methods. Allyn & Bacon (1989)
11. Hesch, C., Glas, S., Schuss, S.: Space-time rigid multibody dynamics. Multibody Syst. Dyn. **61**, 415–434 (2023). https://doi.org/10.1007/s11044-023-09945-1
12. Kinon, P.L., Betsch, P.: Conserving integration of multibody systems with singular and non-constant mass matrix including quaternion-based rigid body dynamics. Multibody Syst. Dyn. **63**, 303–340 (2024). https://doi.org/10.1007/s11044-024-10001-9

13. Kinon, P., Betsch, P., Schneider, S.: The GGL variational principle for constrained mechanical systems. Multibody Syst. Dyn. **57**(3–4), 211–236 (2023). https://doi.org/10.1007/s11044-023-09889-6
14. Kinon, P., Betsch, P., Schneider, S.: Structure-preserving integrators based on a new variational principle for constrained mechanical systems. Nonlinear Dyn. **111**, 14231–14261 (2023). https://doi.org/10.1007/s11071-023-08522-7
15. Krysl, P.: Explicit momentum-conserving integrator for dynamics of rigid bodies approximating the midpoint Lie algorithm. Int. J. Numer. Methods Eng. **63**(15), 2171–2193 (2005). https://doi.org/10.1002/nme.1361
16. Kunkel, P., Mehrmann, V.: Differential-Algebraic Equations. European Mathematical Society (2006)
17. Lens, E., Cardona, A., Géradin, M.: Energy preserving time integration for constrained multibody systems. Multibody Syst. Dyn. **11**(1), 41–61 (2004). https://doi.org/10.1023/B:MUBO.0000014901.06757.bb
18. Leyendecker, S., Marsden, J., Ortiz, M.: Variational integrators for constrained dynamical systems. Z. Angew. Math. Mech. **88**(9), 677–708 (2008)
19. Marsden, J.E., Ratiu, T.S.: Introduction to Mechanics and Symmetry: A Basic Exposition of Classical Mechanical Systems. Springer, New York (1994)
20. Nielsen, M.B., Krenk, S.: Conservative integration of rigid body motion by quaternion parameters with implicit constraints. Int. J. Numer. Methods Eng. **92**(8), 734–752 (2012). https://doi.org/10.1002/nme.4363
21. Nikravesh, P.: Computer-Aided Analysis of Mechanical Systems. Prentice-Hall (1988)
22. Rabier, P., Rheinboldt, W.: Nonholonomic Motion of Rigid Mechanical Systems from a DAE Viewpoint. SIAM, Philadelphia (2000). https://doi.org/10.1137/1.9780898719536
23. Simo, J.C., Wong, K.K.: Unconditionally stable algorithms for rigid body dynamics that exactly preserve energy and momentum. Int. J. Numer. Methods Eng. **31**(1), 19–52 (1991). https://doi.org/10.1002/nme.1620310103
24. Solà, J., Deray, J., Atchuthan, D.: A micro Lie theory for state estimation in robotics. Tech. Rep. IRI-TR-18-01, Institut de Robòticà i Informàtica Industrial, Universitat Politècnica de Catalunya (2018)
25. Ströhle, T., Betsch, P.: A simultaneous space-time discretization approach to the inverse dynamics of geometrically exact strings. Int. J. Numer. Methods Eng. **123**(11), 2573–2609 (2022). https://doi.org/10.1002/nme.6951
26. Wendlandt, J.M., Marsden, J.E.: Mechanical integrators derived from a discrete variational principle. Phys. D: Nonlinear Phenom. **106**(3), 223–246 (1997). https://doi.org/10.1016/S0167-2789(97)00051-1